

# Interactions between Astrocytes and the Reward-Attention Circuit: A Model for Attention Focusing in the Presence of Nicotine

Karine Guimarães<sup>a,b,\*</sup>, Daniele Q.M. Madureira<sup>b</sup>, Alexandre L. Madureira<sup>b</sup>

<sup>a</sup>*Laboratory of Neural Systems, Department of Physics, School of Philosophy, Sciences  
and Letters of Ribeirão Preto, University of São Paulo, Ribeirão Preto, Brazil*

<sup>b</sup>*Laboratório Nacional de Computação Científica, Av. Getúlio Vargas 333,  
Petrópolis-RJ, Brazil*

---

## Abstract

Recent studies in neurophysiology suggest that astrocytes—a specific type of glial cells in the central nervous system—perform dynamical signaling, integrating neural inputs and regulating synaptic transmissions. This work presents a mathematical model for bidirectional signaling between astrocytes and neurons, investigating the functional role of such glial cells in a neural network that simulates the influence of nicotine on attentional focus. Considering the neurons' firing frequency as an indicator of analysis, our results indicate that the tripartite synaptic transmission substantially changes the network activity, in comparison to the bipartite synapse. In addition, we show that this effect occurs specifically due to inclusion of astrocytes, corroborating experimental findings that show astrocytes improve of transmission performance in neural networks. Moreover, our simulations contribute to a better understanding of the astrocytary role in brain function and of synaptic transmission in a neuroglia network.

*Keywords:* Astrocyte, Nicotine, Dopamine, Attention, Computational neuroscience

---

\*Corresponding author

*Email addresses:* [kdamasio@lncc.br](mailto:kdamasio@lncc.br) (Karine Guimarães), [daniele@lncc.br](mailto:daniele@lncc.br) (Daniele Q.M. Madureira), [alm@lncc.br](mailto:alm@lncc.br) (Alexandre L. Madureira)

## 1. Introduction

Neurons and neural circuits are essential for sensory, motor and behavioral integration, as well as for all the processes underlying emotion, cognition and physiological control. However, in spite of the central role neurons play in such mechanisms, these cells are not alone in the brain systems in charge of maintenance and regulation of neurotransmission.

The importance of glial cells for brain activity has already been indicated by Ramon y Cajal more than a century ago [1], but up to recently they were regarded only as a passive component in synaptic transmission. Throughout the last decade however, a number of studies started to suggest a different scenario. Experimental works show that glial networks, in particular astrocyte networks, actively participate in synaptic signaling. Nowadays, the importance of astrocytes for neural functioning and plasticity is highly accepted [2, 3, 4, 5, 6, 7].

A study in neurons from retinas of Pfrieger and Barres mice [8] showed that, in cultures without glial cells, although presenting a normal and complete structure, the synapses exhibited low spontaneous activity and high error rates during synaptic transmission. On the other hand, in a co-culture with neuroglia, the frequency and amplitude of the post-synaptic currents were potentiated seventy times, the spontaneous currents increased five times, with less faults during transmission. These experiments indicate that neurons by themselves form inefficient synapses, and thus need glial signals to achieve high quality connections and become functional.

The role astrocytes play at the central nervous system was thus redefined and it is well accepted that they work as a third element in the synapses. The coupling between astrocytes and neurons form a connection that allows a chemical communication between such cells: a synapse where three terminals change information—a *tripartite synapse* [9, 10].

Observe that although the propagation of action potentials does not occur in astrocytes, these cells are excitable and able to communicate bidirectionally with neurons and other astrocytes. It happens due to the rising and propagation of  $\text{Ca}^{++}$  waves inside the astrocyte. Such waves induce the release of glial transmitters (glutamate) [10, 11] in the synaptic cleft, as a consequence of a pre-synaptic action potential—see Figure 1. Through the activation of the N-methyl-D-aspartate (NMDA) neural receptor, the glutamate transmitter released by the astrocyte produce slow inward currents, especially at dendritic spines [12, 13].

On other hand, nicotine is considered as the main source of tobacco dependence, due to its affinity to the nicotinic acetylcholine receptor (nAChRs) at the reward brain system [14, 15]. The presence of nicotine intensifies cognitive functions—particularly, attention focusing—in a number of groups, as in non-smoking healthy adults, and patients with pathological conditions such as ADHD [16, 17, 18, 19]. Also, the formation of the attentional focus depends on the cortico-thalamic control [20, 21, 22].

The effect of nicotine on synaptic plasticity has been broadly investigated [23, 24, 25, 26]. Nowadays, synaptic plasticity is considered as the basis for the mechanisms underlying learning and memory [27, 28, 29, 30]. Furthermore, the function of glial cells is essential for the consolidation of some types of memories [31, 32, 33]. Moreover, astrocytes possibly perform a key role in Long Term Potentiation (LTP) and Long Term Depression (LTD) [34, 35], as well as in neural synchronicity [36].

In a previous article [37], we proposed a neurocomputational model—called the Reward-Attention Coupled circuit, or RAC for short—that couples reward and thalamocortical circuits to investigate how the action of nicotine at the reward circuit influences attention focusing. Justified by the existence of synaptic projections from the nucleus accumbens (NAcc) up to the substantia nigra (SN) [38], our hypothesis proposes that nicotine affects the attentional focus through the interaction between reward and thalamocortical circuits. The computational simulations of the RAC circuit provide numerical results describing the action potentials of the neurons that compose the neural network. Each neuron is modeled by a system of differential equations that incorporates the cells' electrophysiological characteristics, both in the presence and absence of nicotine.

Biologically plausible models, realistic and accurate at the cellular level, are essential to capture biophysical mechanisms underlying behavior. In fact, several mathematical models have been proposed to understand the functional role of astrocytes in neuronal dynamics [39, 40, 41]. Here, we specifically address the influence that the absorption of astrocytary glutamate exerts on synapses. Moreover, we study the extensive regulatory capacity of astrocytes, i.e., how they are able to modify neural responses throughout the RAC circuit. Therefore, to further understand the dynamical and coordinated interactions between reward and thalamocortical circuits, we present a mathematical model for the bidirectional communication between an astrocyte and the RAC circuit, as well as the computational simulations of this model.

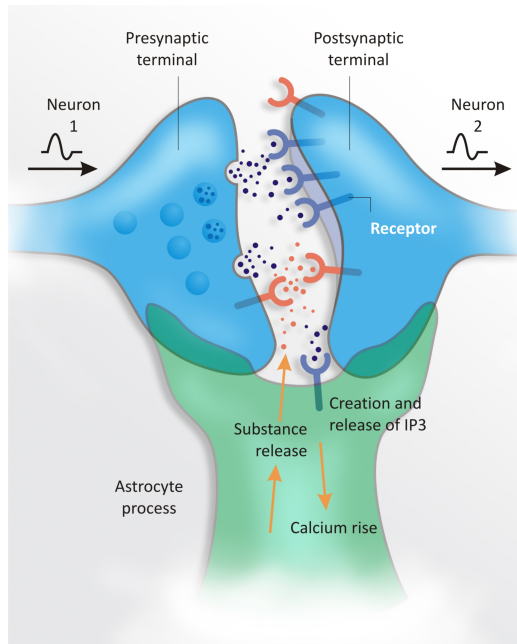


Figure 1: Tripartite Synapse. Pre-synaptic terminal (neuron 1) releases the neurotransmitter glutamate in the synaptic cleft. Glutamate binds to the post-synaptic glutamatergic receptors (neuron 2) and to glutamatergic receptors in the astrocyte. The presence of the neurotransmitter thus triggers a  $\text{Ca}^{++}$  wave inside the astrocyte that, in turn, can release even more glutamate (in this case, a gliotransmitter) than the post-synaptic neuron.

In what follows, we summarize the contents of this article. In Section 2, *Materials and Methods*, we present both the neurophysiology and the mathematical formulation of the RAC-Astrocyte model. In Section 3, *Results*, we describe the computational simulations and present their outcomes. Finally, Section 4 discusses the consequences of our results.

## 2. Materials and Methods

Based on the model proposed by Nadkarni and Jung [39], we investigate the dynamics of the regulation that astrocytes exercise on a neural network. This approach is based on Li and Rinzel  $\text{Ca}^{++}$  model [42] that describes the dynamics of the intracellular  $\text{Ca}^{++}$  waves produced by astrocytes. This model has been particularly developed to consider the  $\text{IP}_3$ -dependent dynamical alterations in the concentration of cytosolic  $\text{Ca}^{++}$ .

### 2.1. Astrocyte-Neuron Interactions

As mentioned before, the interaction between neurons and astrocytes occurs through a tripartite synapse. There, the astrocyte connects to the axonic terminal of the pre-synaptic neuron and to the dendrite of the post-synaptic cell. In this way, the astrocyte modulates the neural signaling according to the stimulus it receives from the pre-synaptic neuron [10].

The astrocyte adjoining the synaptic terminal answers a neural action potential because the released neurotransmitter, glutamate, binds to its receptors, mGluRs receptors type 1 and 5 [43]. The activation of these receptors triggers the production of the  $\text{IP}_3$  second messenger, which regulates the  $\text{Ca}^{++}$  concentration inside the astrocyte.

The  $\text{IP}_3$  production inside the astrocyte is modeled by the following dynamical equation:

$$\begin{cases} \frac{d\text{IP}_3}{dt} = \frac{\text{IP}_3^* - \text{IP}_3}{\tau_{\text{IP}_3}} + \varphi_{\text{IP}_3} \Theta(V - \vartheta) & \text{for } t \in (0, T], \\ \text{IP}_3(0) = \text{IP}_3^0, \end{cases} \quad (1)$$

where  $\text{IP}_3$  represents the amount of  $\text{IP}_3$  in the cytoplasm, and  $\text{IP}_3^*$  is the equilibrium concentration of  $\text{IP}_3$ —which is the basal level of  $\text{IP}_3$  in the cytoplasm when the cell is under a steady state and does not receive inputs. The quantity  $\tau_{\text{IP}_3}$  is the  $\text{IP}_3$  decomposition time constant, and  $\varphi_{\text{IP}_3}$  is the rate through which the  $\text{IP}_3$  is produced due to a neural action potential. The value of  $\text{IP}_3$  at time zero is given by  $\text{IP}_3^0$ .

When the membrane potential  $V$  of the neuron becomes higher than the fixed threshold  $\vartheta$ , the production term is activated through the Heaviside function  $\Theta : \mathbb{R} \rightarrow \{0, 1\}$ , defined as

$$\Theta(x) = \begin{cases} 1 & \text{if } x \geq 0, \\ 0 & \text{if } x < 0. \end{cases} \quad (2)$$

As the intracellular  $\text{IP}_3$  production is proportional to the amount of activated mGluRs, the parameter  $\varphi_{\text{IP}_3}$  is proportional to the amount of neurotransmitter that is released. From (1), we note that  $\text{IP}_3$  oscillates depending on  $V$  while the pre-synaptic neuron is excited. Besides, the frequency of  $\text{IP}_3$  behaves accordingly to the pre-synaptic neuron spiking frequency (see for instance Figure 4a).

## 2.2. Astrocyte $\text{Ca}^{++}$ Dynamics

The  $\text{Ca}^{++}$  dynamics in the Li–Rinzel model is described by three channels:  $\mathcal{J}_{\text{chan}}$ , which models the  $\text{Ca}^{++}$  influx from the endoplasmic reticulum (ER) up to the cytoplasm, through the opening of both  $\text{IP}_3$  and  $\text{Ca}^{++}$  channels;  $\mathcal{J}_{\text{pump}}$ , which models the influx of  $\text{Ca}^{++}$  that is pumped from the extracellular space up to the ER; and finally,  $\mathcal{J}_{\text{leak}}$ , which describes the amount of  $\text{Ca}^{++}$  that leaks through the membrane of the ER to the cytoplasm. Thus, the cytoplasmic  $\text{Ca}^{++}$  concentration is described by the following system of equations (see [41] for a complete derivation):

$$\begin{cases} \frac{d[\text{Ca}]}{dt} = \mathcal{J}_{\text{chan}}([\text{Ca}], q, \text{IP}_3) + \mathcal{J}_{\text{pump}}([\text{Ca}]) - \mathcal{J}_{\text{leak}}([\text{Ca}]) & \text{for } t \in (0, T] \\ \frac{dq}{dt} = \alpha_q(1 - q) - \beta_q q & \text{for } t \in (0, T] \\ [\text{Ca}](0) = [\text{Ca}]^0, \quad q(0) = q^0, \end{cases}$$

where  $\mathcal{J}_{\text{chan}}$  depends on the states of the  $\text{IP}_3$  and  $\text{Ca}^{++}$  channels,  $\mathcal{J}_{\text{pump}}$  and  $\mathcal{J}_{\text{leak}}$  depend on the  $\text{Ca}^{++}$  concentration,  $q$  is the fraction of activated  $\text{IP}_3$  receptors, and the parameters  $\alpha_q$  and  $\beta_q$  are given by

$$\alpha_q = a_2 d_2 \frac{\text{IP}_3 + d_1}{\text{IP}_3 + d_3}, \quad \beta_q = a_2 [\text{Ca}].$$

The description of the channel  $\mathcal{J}_{\text{chan}}$  is

$$\mathcal{J}_{\text{chan}} = r_c m_\infty^3 n_\infty^3 q^3 ([\text{Ca}] - [\text{Ca}]_{\text{RE}}),$$

where  $r_c$  is the  $\text{Ca}^{++}$  maximum rate of oscillation and propagation. Besides,  $m_\infty$  and  $n_\infty$  are the  $\text{IP}_3$  and  $\text{Ca}^{++}$  channels respectively, which are described by

$$m_\infty = \frac{\text{IP}_3}{\text{IP}_3 + d_1}, \quad n_\infty = \frac{[\text{Ca}]}{[\text{Ca}] + d_5}.$$

The other channels,  $\mathcal{J}_{\text{leak}}$  and  $\mathcal{J}_{\text{pump}}$ , are given by

$$\mathcal{J}_{\text{pump}} = \nu_{\text{RE}} \frac{[\text{Ca}]^2}{\kappa_{\text{RE}}^2 + [\text{Ca}]^2}, \quad \mathcal{J}_{\text{leak}} = r_L ([\text{Ca}] - [\text{Ca}]_{\text{RE}}),$$

where  $r_L$  is the  $\text{Ca}^{++}$  leaking rate,  $\nu_{\text{RE}}$  is the pump's maximum rate of absorption, and  $\kappa_{\text{RE}}^2$  is the constant for the activation of the pump. Table 1 presents a complete description of all parameters. Important to note, for

the conservation of the  $\text{Ca}^{++}$  concentration inside the cell, the restriction  $[Ca]_{\text{RE}} = \frac{c_0 - [Ca]}{c_1}$  must be satisfied, where  $c_0$  represents the overall concentration of free cytosolic  $\text{Ca}^{++}$  and  $c_1$  is the volumetrical rate between the ER and the cytoplasm.

Table 1: Astrocyte Parameters

Parameters	Description	Value
$\text{IP}_3^*$	Baseline value of $\text{IP}_3$	$0.16 \mu\text{M}$
$\tau_{\text{IP}_3}$	$\text{IP}_3$ degradation time constant	$7 \text{ s}$
$\varphi_{\text{IP}_3}$	Production rate for $\text{IP}_3$	$7.2 \mu\text{M s}^{-1}$
$\vartheta$	Threshold for the $\text{IP}_3$ production	$50 \text{ mV}$
$r_c$	Maximum rate for the oscillation and propagation of $\text{Ca}^{++}$	$6 \text{ s}^{-1}$
$r_L$	$\text{Ca}^{++}$ leakage rate from ER	$0.11 \text{ s}^{-1}$
$\nu_{\text{RE}}$	Maximum rate for the $\text{Ca}^{++}$ pump uptake	$0.9 \mu\text{M s}^{-1}$
$c_0$	Total free $\text{Ca}^{++}$ cytosol concentration	$2 \mu\text{M}$
$\kappa_{\text{RE}}^2$	Activation constant for the $\text{Ca}^{++}$ pump	$0.1 \mu\text{M}$
$c_1$	Ratio of ER volume to cytosol volume	$0.185$
$d_1$	$\text{IP}_3$ dissociation constant	$0.13 \mu\text{M}$
$d_2$	$\text{Ca}^{++}$ inactivation dissociation constant	$1.049 \mu\text{M}$
$d_3$	$\text{IP}_3$ dissociation constant	$0.9434 \mu\text{M}$
$d_5$	$\text{Ca}^{++}$ activation dissociation constant	$0.08234 \mu\text{M}$
$a_2$	Rate for the binding and inactivation of $\text{IP}_3$ and $\text{Ca}^{++}$	$0.2 \mu\text{M s}^{-1}$

### 2.3. Neuron Model

The neural modeling applied to the RAC circuit is described in detail in [37]. For completeness we summarize here the main aspects of the network.

In our model, the reward system is activated by the action of nicotine on  $\alpha_7$  receptors at the axonic terminals of neurons in the pre-frontal cortex (PFC). Such neurons release glutamate to the ventral tegmental area (VTA), which nicotinic and glutamatergic receptors are activated by nicotine and glutamate, respectively. By this way, the dopaminergic and GABA-ergic neurons in the VTA become excited. The activity of the GABA-ergic neurons, however, ends after some minutes, due to properties of their nicotinic receptors. The dopaminergic neurons, on the other hand, keep receiving excitatory stimuli from the glutamatergic PFC neuron, while the inhibitory stimuli

from the GABA-ergic neurons die out. As a consequence LTP occurs, mediated by the glutamatergic receptor NMDA. Such sequence of events makes the dopaminergic neurons to spike under the burst mode, releasing more dopamine. These cells make connections with GABA-ergic neurons at the NAcc, the last site in the reward pathway related to the pleasure sensation induced by the use of nicotine.

The NAcc inhibits the dopaminergic neurons in the SN, which connects the reward and the thalamocortical circuits. Since the NAcc projections are inhibitory, the SN and NAcc behaviors are inversely proportional, i.e. the SN becomes more (less) active as the NAcc becomes more (less) inhibited.

We now consider the thalamocortical part of the RAC-Astrocyte model, where  $T_x$  and  $T_y$  are two neighboring thalamic regions, and the inputs  $x$ ,  $y$  represent external stimuli that activate  $T_x$  and  $T_y$  through glutamatergic excitatory connections.

When stimulated,  $T_x$  sends excitatory signals to the TRN through a glutamatergic projection that ends in the PFC. In this article, we do not explicitly model the cortical area in the thalamocortical circuit. Here therefore the modeled projection departing from  $T_x$  ends up in the TRN. On the other hand, this cortical region sends an excitatory glutamatergic descending projection to  $T_x$ , through which it increases the activation of  $T_x$ , and also sends collateral axons to the TRN. If activated, a GABA-ergic TRN projection inhibits  $T_y$ . This model represents a TRN neuron stimulated by one neuron from the thalamic region  $T_x$  and another from the PFC. This mechanism underlies the generation of an attentional focus (for further details see [22]).

Since the SN sends dopaminergic inhibitory projections to the TRN, a rise in the level of dopamine released by the SN contributes for the deactivation of the TRN. As a consequence, the thalamic region  $T_y$  becomes more active and the attentional focus more flexible. However, a decrease in the SN dopaminergic level makes the TRN more excited and  $T_y$  more inhibited. In this situation, the attention loses its flexibility and becomes much more focused on the stimulus  $x$ .

Summarizing, through our model we propose that the behavior of the SN, which suffers influence from the NAcc, modulates the focusing of attention. And the action of nicotine is powerful enough to affect the level of activity at the NAcc.

Given the role of the synaptic plasticity in mediating the action of psychoactive substances, we investigate the influence of astrocytes on synapses between the pre-synaptic glutamatergic and the post-synaptic dopaminergic

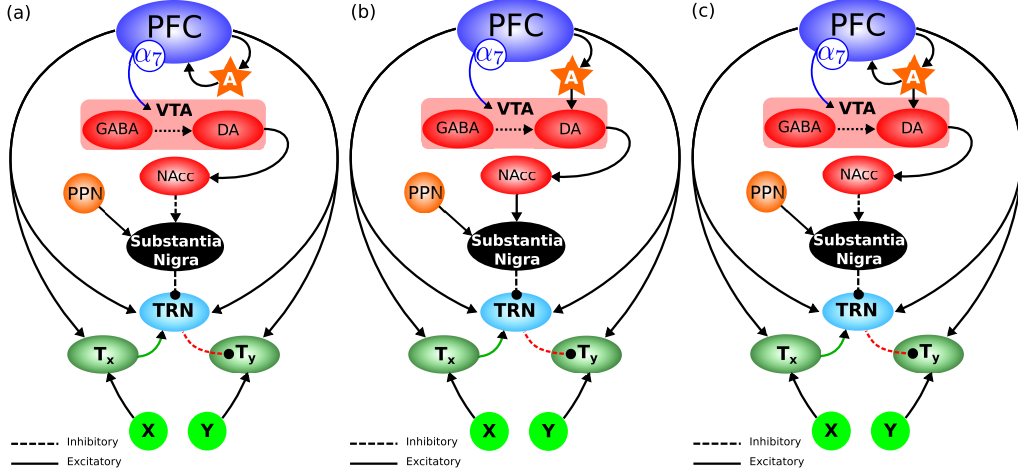


Figure 2: Reward Attention Circuit architecture: excitatory synapses (continuous lines), inhibitory synapses (dotted lines). Here, the reward circuit is represented by the pre-frontal cortex (PFC), and the ventral tegmental area (VTA) and nucleus accumbens (NAcc) regions. The thalamocortical circuit includes the PFC, thalamus and the thalamic reticular nucleus (TRN). The communication between these circuits is established through the substantia nigra (SN) that inhibits the TRN and receives inhibitory projections from the NAcc. The pedunculopontine nucleus (PPN), in turn, excites the SN. The star depicts the astrocyte. (a) Case 1: Feedback mode; (b) Case 2: Gliotransmitters act on the post-synaptic neuron; (c) Case 3: Gliotransmitters act both on the pre-synaptic and post-synaptic neurons.

neurons at the reward circuit, as we observe in Figures 2(a-c). Accordingly, whenever glutamate is released in the synaptic cleft, this transmitter binds to receptors in the post-synaptic neuron as well as in the astrocyte. As a consequence of such glutamatergic action in the tripartite synapse, the astrocyte releases its glial transmitters.

The communication between astrocytes and neurons usually occurs under three situations [39]: (1) a feedback mode, where the glial transmitters operate in the pre-synaptic neuron (Figure 2a); (2) glial transmitters act in the post-synaptic neuron (Figure 2b); (3) glial transmitters act in both pre and post-synaptic neurons (Figure 2c). In this work, we analyze these three cases.

To model the behavior of neurons mathematically, we apply an Integrate and Fire approach [44], considering one-compartment neurons with electric potential  $V$  [22, 45, 46, 47, 48]. The membrane of the neuron is modeled by electric capacitors in parallel with a series of resistors, which represent ions

channels and synaptic connections. In general, the membrane equation is described by

$$\begin{cases} C_i \frac{dV_i}{dt} = \sum_{j=1}^{J_i} I_i^j + I_{\text{ext}} & \text{for } t \in (0, T] \text{ and } V_i < \theta_{\text{Na}}, \\ V_i(0) = V_i^0, \end{cases}$$

where  $i = 1, \dots, n$  refers to each of the  $n$  neurons in the network,  $C_i$  denotes their capacitances, and  $J_i$  is the number of ionic currents being modeled in the  $i$ th neuron. The external currents  $I_{\text{ext}}$  are due to eventual influences of the astrocyte, synaptic currents and the presence of nicotine, and will be described further below. Finally,  $\theta_{\text{Na}}$  is a fixed, predefined constant. The currents are defined as  $I_i^j = g_j(V_i)(E_j - V_i)$ , where  $g_j$  is the conductance and  $E_j$  is the Nernst potential corresponding to the  $j$ th ion. The physiological characteristics of each neuron is modeled by the conductance  $g_j$ , which might not only depend on  $t$  explicitly, but also on previous values of  $V_i$  itself, through, for instance, additional differential equations.

We assume that spikes are due to voltage-dependent currents—the sodium current, which depolarizes the neuron, and the potassium current  $I_{\text{K}}$ , which restores the cellular membrane potential—and synaptic currents, which contribute to the excitation or inhibition of the cell, according to the behavior of the pre-synaptic neurons. Also, we consider the leak current, which lumps other currents not explicitly modeled.

As an exception, the sodium current is not represented as described above. It is activated by the action of the Heaviside function defined in (2), applied to  $(V_i - \theta_{\text{Na}})$ .

After a spike, the conductance  $g_{\text{k}}$  of the restoring current  $I_{\text{K}}$  increases rapidly, bringing the neuron back to a resting potential. This process is described in general by

$$\frac{dg_{\text{k}}}{dt} = \frac{\beta_{\text{k}} \Theta(V - \theta_{\text{Na}}) - g_{\text{k}}}{\tau_{\text{k}}} \quad \text{for } t \in (0, T], \quad g_{\text{k}}(0) = g_{\text{k}}^0,$$

where the constants  $g_{\text{k}}^0$ ,  $\beta_{\text{k}}$  and  $\tau_{\text{k}}$  are the initial state of  $g_{\text{k}}$ , the variation rate of  $g_{\text{k}}$ , and the time constant associated with the potassium channel. The above equation actually holds for all neurons, with  $V$  being replaced  $V_i$ ,  $g_{\text{k}}$  replaced by  $g_{\text{k},i}$ , etc.

The external currents  $I_{\text{ext}}$  acting on the  $i$ th neuron can be given by synaptic currents of the form  $g_{\text{syn}}(t)(E_{\text{syn}} - V_i)$ , by  $\alpha_7^+$  (see (3)) due to the presence of nicotine, and by astrocyte currents as in (5).

The synaptic conductances  $g_{\text{syn}}$  reflect the level of a neurotransmitter released by the pre-synaptic neuron, being described by

$$g_{\text{syn}}(t) = \hat{g}_{\text{syn}} \sum_j (t - t_j) \exp\left(-\frac{t - t_j}{t_p}\right) \Theta(t - t_j),$$

where the times  $t_j$ , with  $j = 1, \dots, \mathcal{N}$ , are the spiking times of a pre-synaptic cell, while the constant  $\hat{g}_{\text{syn}}$  is the maximal conductance. We denote by  $t_p$  the peak time for the alpha function, and it assumes the values  $t_{pe}$  and  $t_{pi}$  for excitatory and inhibitory synapses, respectively.

All the neurons in the network present sodium and potassium ionic currents, and synaptic currents. However, each neuron receives distinct neurotransmitters according to their specific afferents. Besides the currents involved in the action potential, there are those associated with particular properties of each neuron. For example, nicotine acts on the cortical neuron through the  $\alpha_7$  receptors. The variation in the number of activated  $\alpha_7^+$  receptors is given by the solution of the equation

$$\frac{d\alpha_7^+}{dt} = k_1 \alpha_7^- n_{ic} - k_2 \alpha_7^+ \quad \text{for } t \in (0, T], \quad \alpha_7^+(0) = \alpha_7^{+,0}, \quad (3)$$

where  $\alpha_7^{+,0}$ ,  $\alpha_7^-$ ,  $k_1$  and  $k_2$  are constants, and  $n_{ic} : (0, T] \rightarrow \mathbb{R}$  is solution for the following differential equation

$$\frac{dn_{ic}}{dt} = -M n_{ic} \quad \text{for } t \in (0, T], \quad n_{ic}(0) = n_{ic}^0, \quad (4)$$

where  $M$  e  $n_{ic}^0 \in \mathbb{R}$ . So, besides ionic currents, the cortical neuron also holds a term representing the amount of activated alpha receptors.

On other hand, astrocytes modulate the synaptic information in response to increases in their intracellular  $\text{Ca}^{++}$  concentration. When the level of the  $\text{Ca}^{++}$  concentration surpasses a defined threshold  $[Ca]_{\text{thres}} \in \mathbb{R}$ , the astrocyte releases glial transmitters and generates a slow current inside the neuron. This current is described as

$$I_{\text{ast}} = \kappa \Theta(\ln([Ca] - [Ca]_{\text{thres}})) \ln([Ca] - [Ca]_{\text{thres}}), \quad (5)$$

where  $\kappa \in \mathbb{R}$  e  $\Theta$  is the Heaviside function defined in (2).

Several works report situations where the glutamate, which is released by astrocytes and acts on NMDARs at postsynaptic neurons, triggers slow

currents SICs [13, 49, 50, 51]. These results, however, are not yet completely confirmed in the VTA and PFC. Therefore, here, we employ the same kind of astrocytary current in the pre and postsynaptic neurons.

The differential equations are discretized in time using the Euler’s method. For a more detailed information about the neuron model, including all equations and parameters values, see [37].

### 3. Simulation methods

Prior to conducting experiments to address the network behavior, we calibrate each neuron separately, according to their specific neurophysiological properties [37]. Next, we start our simulations considering a “healthy” brain, and set the physiological parameters in the “normal” range [21, 22, 37, 53], an essential step to establish benchmark results. By healthy, we mean an individual with no pathology, whose brain has not been exposed to nicotine ( $n_{ic}^0 = 0$  in (4)) and with a normal capacity of attentional focusing. For a normal attentional focus on stimulus  $x$  to occur, the thalamic area  $T_x$  must be more activated than its neighboring area  $T_y$ . However, it is also necessary that the amount of activation in  $T_y$  is not much lower than the one occurring in  $T_x$  — otherwise, there will appear an hyper attention focusing on  $x$  (see Figure 3). Besides, the activation of  $T_y$  cannot be similar to  $T_x$  — otherwise, there will be no attention focusing at all [22].

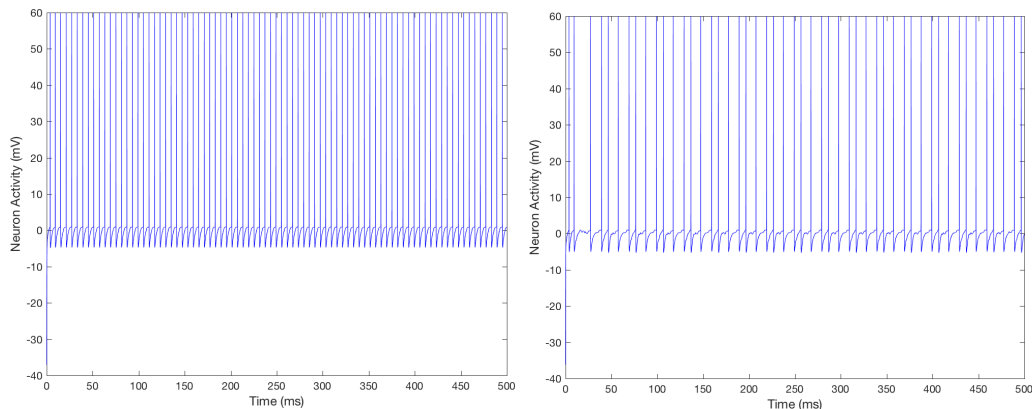


Figure 3: Attention focusing in a healthy individual, without nicotine: (a) Behavior of  $T_x$ ; (b) Behavior of  $T_y$ .

We consider that at the baseline case the reward system remains almost

inactive, in the absence of nicotine. Next, we designed an experiment addressing the case involving exposure to nicotine. Starting from the baseline case, nicotine is added to the system by imposing  $n_{ic}^0 \neq 0$  in (4). All other parameters are the same as in the baseline case [37].

## 4. Numerical results

### 4.1. Case 1: PFC-Astrocyte Bidirectional Communication

In this first case, we assume that the astrocyte communicates solely with the PFC neuron. Under the a nicotinic input, the PFC neuron starts to stimulate the astrocyte. By its turn, the glial cell sends a signal back to the neuron, thus strengthening this neuron-astrocyte communication.

To provide a better visualization of the  $IP_3$  evolution and the  $Ca^{++}$  wave oscillations, Figure 4(a) shows the  $IP_3$  evolution, and Figure 4(b) presents the resulting oscillation of the  $Ca^{++}$  concentration due to the pre-synaptic glutamatergic stimulation.

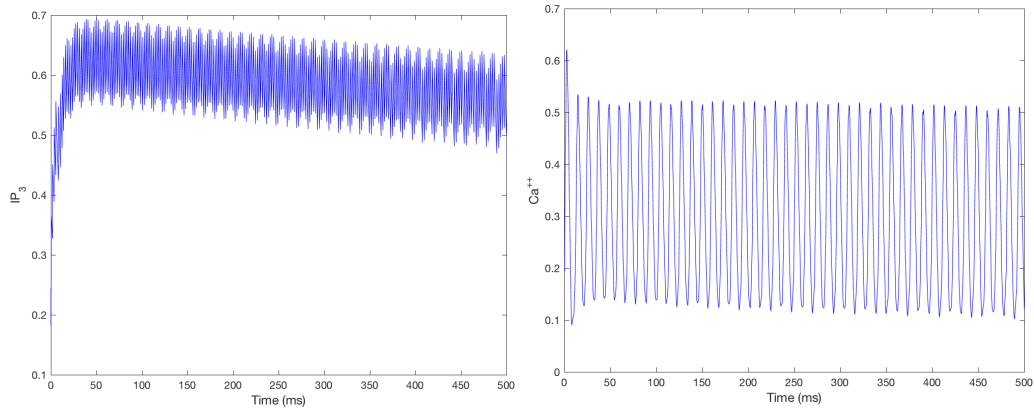


Figure 4: Case 1: (a)  $IP_3$  evolution; (b)  $Ca^{++}$  oscillation.

Regarding the RAC circuit simulations, we note that the strengthening of the PFC neuron excitatory state, promoted by the astrocyte action, presents a particular influence on the synaptic projection to the VTA dopaminergic neuron. Figure 5 shows the behavior of such neuron without and with the astrocytary regulatory role.

We can observe that the behavior of both VTA dopaminergic neurons is qualitatively similar in both situations, since they at first spike under the tonic mode and then turn to the burst state. We note however that the

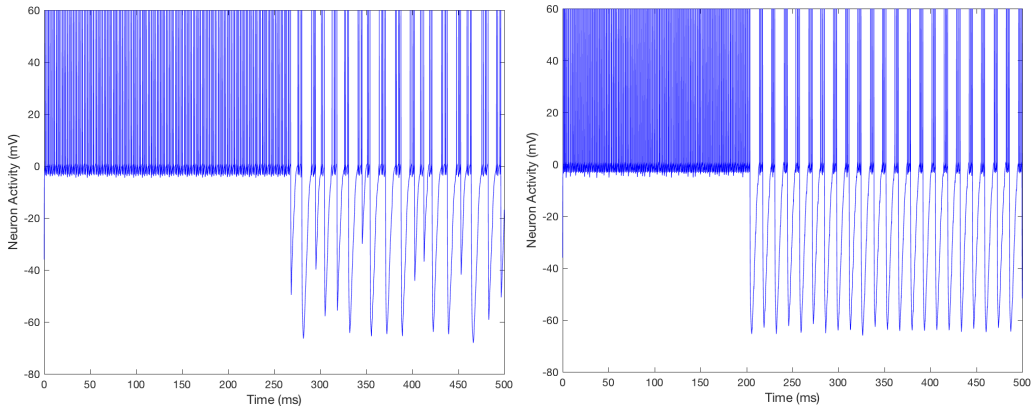


Figure 5: Case 1: (a) Action potential of the VTA dopaminergic neuron in the RAC-circuit; (b) Action potential of the VTA dopaminergic neuron in the RAC-Astrocyte circuit.

spikes become more regular under presence of the glial cell. Indeed, the VTA dopaminergic neuron turns to the burst mode earlier, and its hyperpolarizations are more even under the astrocytary action.

Figure 6 displays, for this Case 1, the attentional focus formation, both in the RAC and the RAC-Astrocyte circuits, through the spikes of the thalamic neurons  $T_x$  e  $T_y$ .

In the beginning of the simulation, the presence of nicotine promotes a hyper focused attention that turns into cognitive flexibility as the simulation proceeds.

We also note that, without the astrocyte, the system is more resistant to return to its basal state. In this case, up to 110ms there occurs an extreme attentional hyper focusing, which is followed by a high focused attention. In what follows, around 280ms the system tends to reach its basal state and the attention becomes less highly focused.

On the other hand, in the RAC-astrocyte circuit the hyper focusing state lasts longer, around 210 milliseconds. Then, the cognitive flexibility comes up, as the thalamic neurons behavior becomes similar to their basal state.

This experiment shows the regulatory role of the astrocyte and suggests that synaptic efficacy depends on the astrocytary function.

#### 4.2. Case 2: PFC-Astrocyte-VTA Communication

In the present case, the astrocyte receives inputs from the PFC neuron, as in Case 1, but its response is directed to the VTA dopaminergic neuron. As

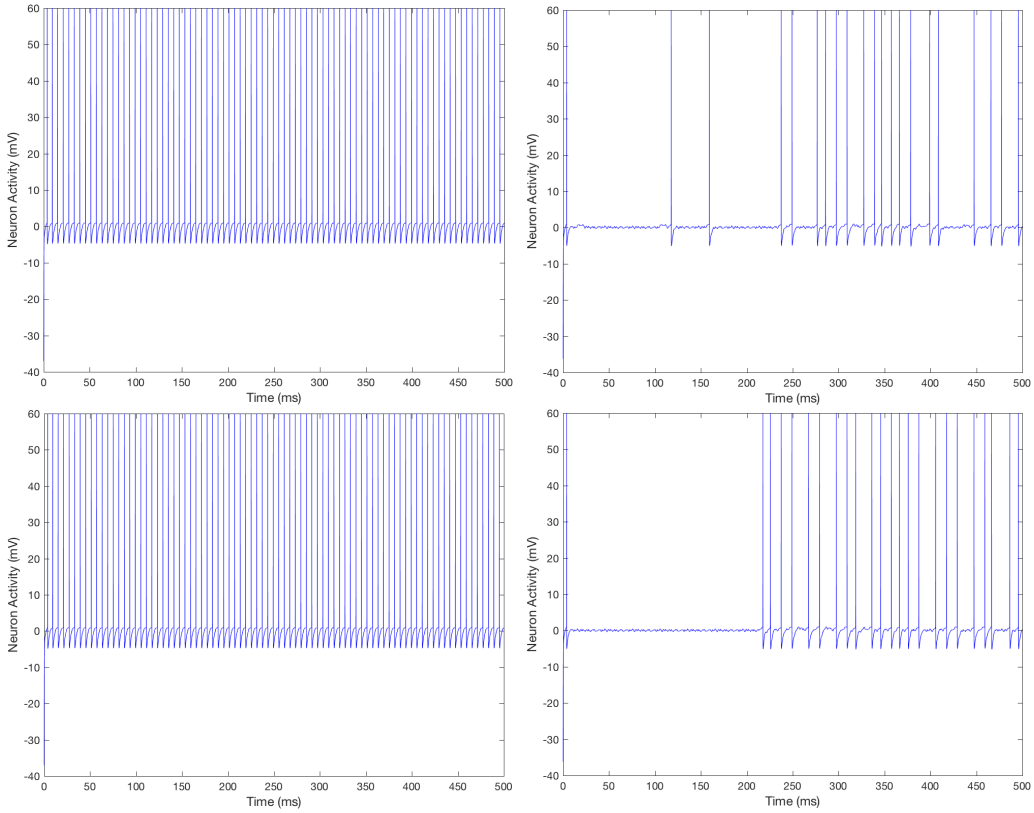


Figure 6: Case 1: Attention focusing in the RAC and RAC-Astrocyte circuits. (a)  $T_x$  in the RAC circuit; (b)  $T_y$  in the RAC circuit; (c)  $T_x$  in the RAC-Astrocyte circuit; (d)  $T_y$  in the RAC-Astrocyte circuit.

in the previous experiment, nicotinic stimulus in the PFC neuron activates the RAC circuit and the astrocyte. The glial cell responds to such activation, and sends an input signal to the VTA dopaminergic neuron.

Figures 7(a,b) represent, respectively, the graphics for the variation of  $IP_3$  and the  $Ca^{++}$  oscillation. And in Figures 8(a,b), we observe the action potentials of the dopaminergic neuron in the RAC and RAC-Astrocyte circuits, respectively. Note that, in this case, the dopaminergic neuron at the RAC-astrocyte circuit also spikes under the burst mode a slightly earlier than at the RAC circuit and, in addition, its frequency of hyperpolarizations is higher than in the RAC circuit simulation. Finally, Figure 9 presents the spikes of  $T_x$  and  $T_y$ , in RAC and RAC-Astrocyte circuits.

Due to the increase in the activation of the VTA dopaminergic neuron,

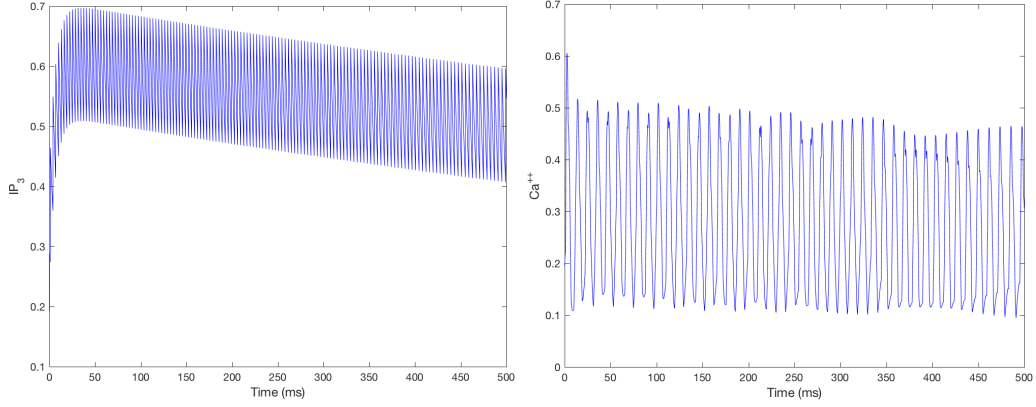


Figure 7: Case 2: (a) IP<sub>3</sub> evolution; (b) Ca<sup>++</sup> oscillation.

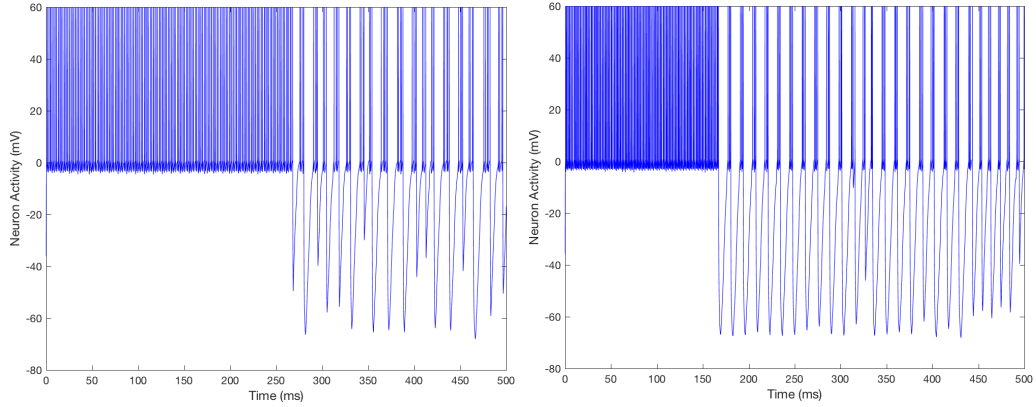


Figure 8: Case 2: (a) Action potential of the VTA dopaminergic neuron in the RAC-circuit; (b) Action potential of the VTA dopaminergic neuron in the RAC-Astrocyte circuit.

which was promoted by the astrocytary current, there is an increase in the activity of the NAcc neuron. Such situation makes the SN highly inhibited during the first 150 milliseconds.

As a consequence of the low dopaminergic activity in the SN, the TRN markedly inhibits  $T_y$  and the attentional focus becomes completely concentrated on the stimulus  $x$ . When the VTA dopaminergic neuron starts to spike under the burst mode, the attentional focus turns to be more flexible, and the behavior of  $T_y$  goes back to normality.

In this case, the comparison between the attention focusing in the RAC and in the RAC-Astrocyte circuits reveals that the system returns to the

basal situation faster than in the RAC network simulation, in presence of the astrocyte.

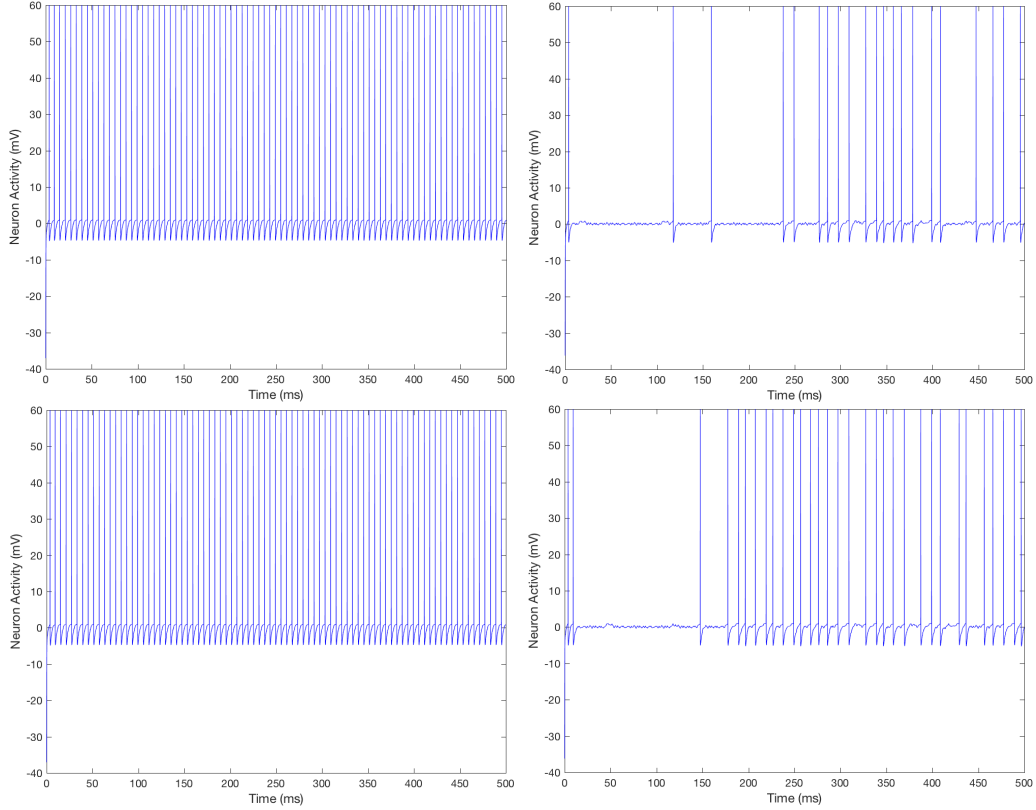


Figure 9: Case 2: Attention focusing in the RAC and RAC-Astrocyte circuits. (a)  $T_x$  in the RAC circuit; (b)  $T_y$  in the RAC circuit; (c)  $T_x$  in the RAC-Astrocyte circuit; (d)  $T_y$  in the RAC-Astrocyte circuit.

#### 4.3. Case 3: PFC-Astrocyte Bidirectional Communication and PFC-Astrocyte-VTA Communication

This third case combines modeling characteristics of Cases 1 and 2, in the sense that the astrocyte receives inputs from the PFC neuron nicotinic stimulated, and responds to both the PFC and the VTA dopaminergic neuron. The glial cell responds to such activation through its bidirectional communication with the cortical neuron, and through its connection with the VTA dopaminergic neuron.

Figures 10(a-b) depict the respective  $IP_3$  evolution and resulting  $Ca^{++}$  oscillation. In the sequence, Figures 11(a,b) show the action potentials of the dopaminergic neuron in the RAC and RAC-Astrocyte circuits, according to this Case 3 conditions.

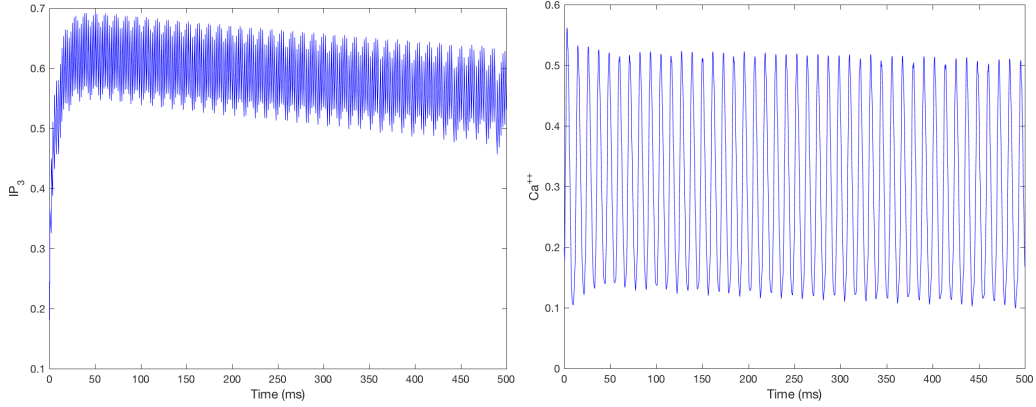


Figure 10: Case 3: (a)  $IP_3$  evolution; (b)  $Ca^{++}$  oscillation.

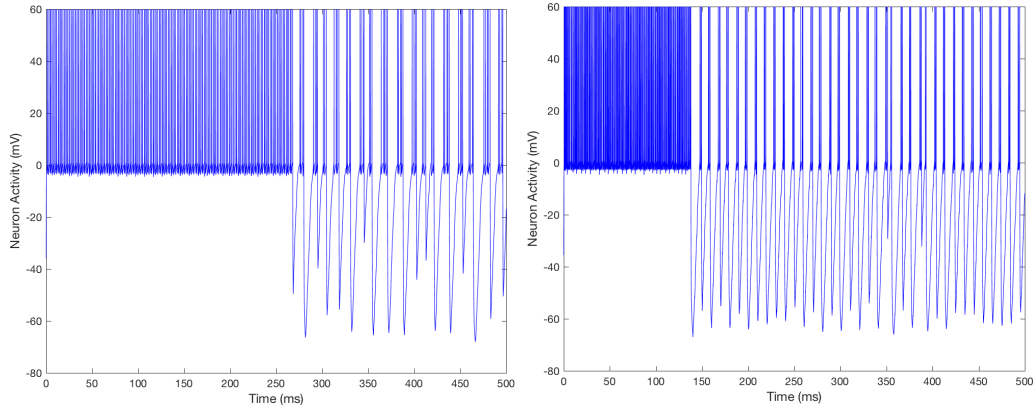


Figure 11: Case 3: (a) Action potential of the VTA dopaminergic neuron in the RAC-circuit; (b) Action potential of the VTA dopaminergic neuron in the RAC-Astrocyte circuit.

Here it is also possible to note that the dopaminergic neuron in the RAC-Astrocyte circuit starts to spike under the burst mode around 100 milliseconds earlier than in the RAC simulation, with a higher frequency of its hyperpolarizations. Figure 12 presents the spikes of  $T_x$  and  $T_y$  in the RAC and RAC-astrocyte circuits.

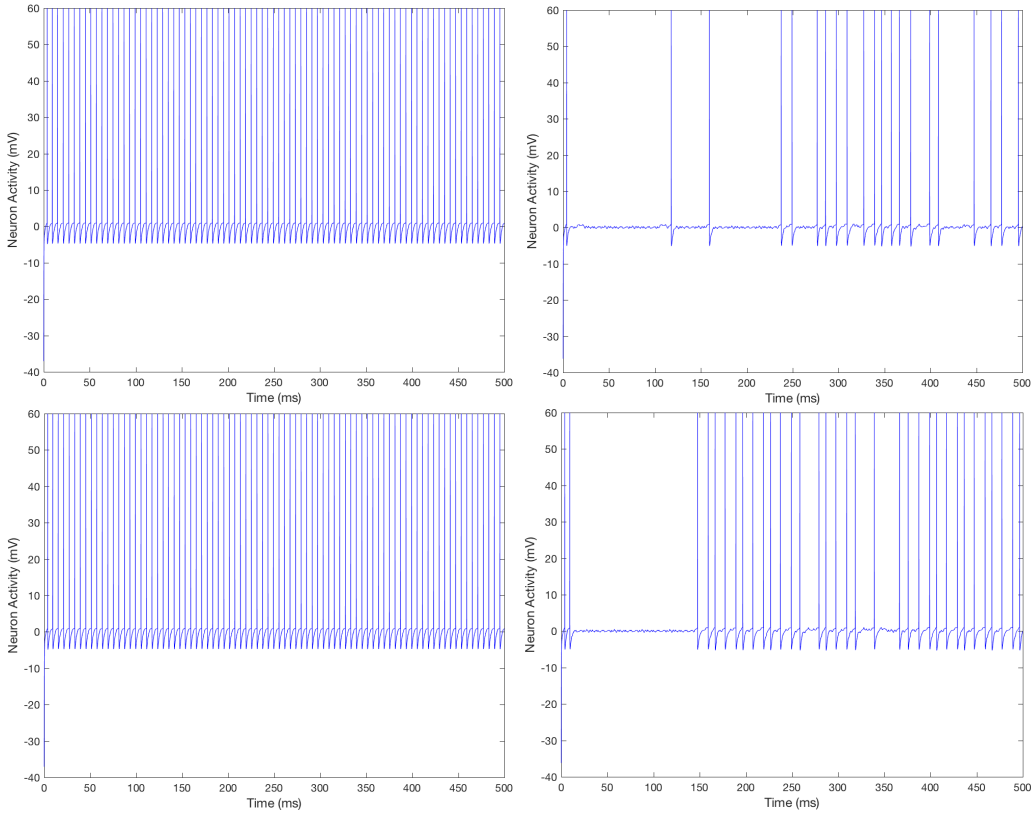


Figure 12: Case 3: Attention focusing in the RAC and RAC-Astrocyte circuits. (a)  $T_x$  in the RAC circuit; (b)  $T_y$  in the RAC circuit; (c)  $T_x$  in the RAC-Astrocyte circuit; (d)  $T_y$  in the RAC-Astrocyte circuit.

The output of this experiment is similar to the results shown in Case 2. After around a 150 millisecond hyper focused attention, we note the appearance of cognitive flexibility, since the thalamic neurons' behavior returns to the basal state.

Once again, we highlight the astrocytary regulatory function. Compared to Cases 2 and 3, the experiment presented in Case 1 illustrates more clearly the literature that report a better signal transmission in presence of astrocytes.

Even so, Cases 2 and 3 simulations also expose enhancements relative to transmission in the VTA dopaminergic neuron. Overall, our simulations evidence the astrocytary modulatory role in the attention focusing mechanism. Moreover, they point that distinct patterns of connectivity at the tripartite

synapse can lead to distinct levels of attentional focus. In particular, the feedback mechanism between the PFC neuron and the astrocyte promotes a more accentuated attention focusing. Conversely, the absence of such bidirectional communication does not produce a marked hyper focusing, since the high concentration on stimulus X is briefer than what we observe in Cases 2 and 3.

#### 4.4. Astrocytary Influence on the Network Performance

After undertaking this series of experiments, we wondered if the improvement in the network performance indicated by our results was specifically related to the astrocyte, or simply due to the presence of another “player”, regardless of its origin.

So, we designed a new experiment to investigate if, by changing the astrocyte by a neuron, the RAC circuit would produce similar improvements. Accordingly, we substituted the astrocyte by a neuron, whose behavior was modeled as a spiking pattern of one spike per millisecond, and considered again the experiments previously described.

In Figures 13(a,b), we can compare the behavior of the VTA dopaminergic neuron above presented in Case 1, with the situation in which the astrocyte is changed by a neuron. In Figure 13(a) the astrocyte is present, while in Figure 13(b) the glial cell is substituted by a neuron. Figures 14 and 15 present the same comparisons for the Cases 2 and 3, respectively.

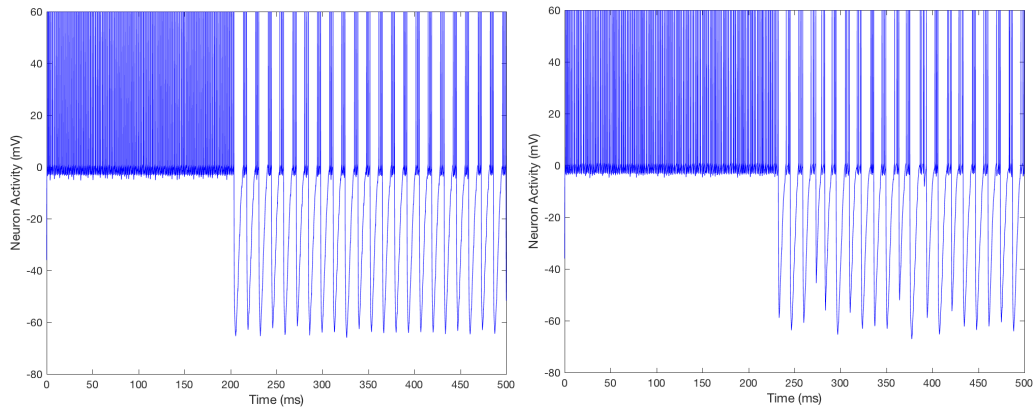


Figure 13: Behavior of the VTA dopaminergic neuron when it is coupled to an astrocyte (a), and coupled to a neuron (b). Both under the Case 1 conditions, as presented in Section 3.1.

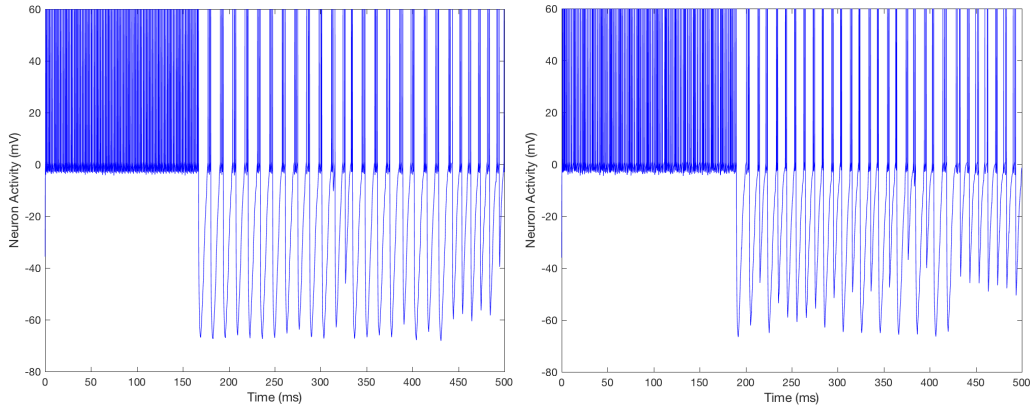


Figure 14: Behavior of the VTA dopaminergic neuron when it is coupled to an astrocyte (a), and coupled to a neuron (b). Both under the Case 2 conditions, as presented in Section 3.2.

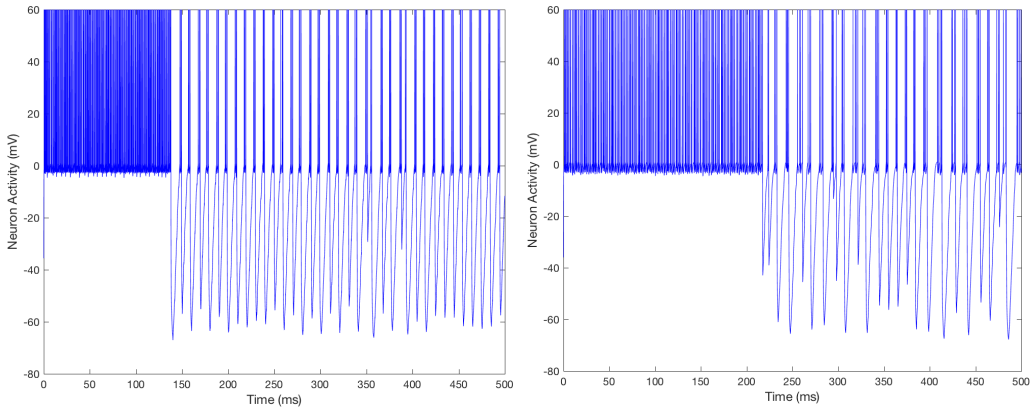


Figure 15: Behavior of the VTA dopaminergic neuron when it is coupled to an astrocyte (a), and coupled to a neuron (b). Both under the Case 3 conditions, as presented in Section 3.3.

We observe clearly that the improvement in the performance of the VTA dopaminergic neuron was not correlated to the increase in the amount of neurons at the network. Therefore, these results reinforce the idea that synaptic efficiency is really dependent on the presence of the astrocyte in the tripartite synapse.

It is important to highlight that the values applied to the neuron-VTA currents are very similar to the values provided by the astrocyte-VTA currents.

## 5. Discussion

The RAC-Astrocyte model we present in this work captures the bidirectional coupling between an astrocyte and the reward-attention circuit, and the computational simulations of this modeling point that indeed astrocytes regulate the transmission of neural signals. Therefore, our results corroborate and support recent experimental studies that propose a direct astrocytary involvement in the information processing throughout the brain [10, 4, 52].

Experimental evidence indicates that astrocytes take part in LTP/LTD mechanisms. Deficiencies in the glial fibrillary protein GFAP, which is expressed predominantly in the astrocytes at the central nervous system, seem to exacerbate LTP, thus impairing the LTD [34, 35]. According to our simulations, increases in both electrical activity and dopamine releasing by the VTA dopaminergic neurons—due to nicotinic stimulus—are highly regulated through the activation of glutamatergic NMDA receptors as a consequence of LTP. Also, the  $\text{Ca}^{++}$  influx and posterior increase in its concentration inside the VTA dopaminergic neuron, which are also related to LTP, amplify the hyperpolarization phase of the cell’s action potential. Important to note, the hyperpolarization is essential for the burst spiking mode to occur [53, 54].

Our results indicate that different kinds of tripartite synapses support different kinds of attentional focus. Such influence, however, might be due to the same approach applied to both pre and postsynaptical release modeling. In this context, an extension of the RAC-Astrocyte model, which includes different approaches to the cellular signaling undertaken by pre and postsynaptical neurons, would provide an even better comprehension of the network functioning.

Moreover, our results indicate that astrocytes do present a modulatory role in the occurrence of neural burst spikes—a mode of spiking associated to dopamine release in rewarding situations. Therefore, this work highlights the importance of the tripartite synapse, supporting the notion that neuron-glia interactions undertake a synchronized communication.

As the presence of the astrocyte influenced even the thalamic behavior, it is plausible to emphasize its importance to the overall network performance. Moreover, our results suggest that the synaptic efficacy depends on its relation with the astrocytary cell, since the substitution of the astrocyte by a neuron led to different results when compared to those under the presence of the glial cell.

The results of our study reinforce the hypothesis that astrocyte networks

provide much more than a structural support for neural networks. They indicate in particular the role of astrocytes in mechanisms underlying the focusing of attention in presence of nicotine.

## Acknowledgments

We gratefully acknowledge Diego Paredes for the help with the figures. The first author acknowledges the Brazilian agency CNPq for the financial support, grant numbers 168208/2014-8, 454815/2015-8 and 151006/2017-2. The second author thanks the Laboratório Nacional de Computação Científica for the hospitality. The third author acknowledges the financial support from CNPq, grants 232677/2014-0 and 312963/2014-9.

## References

- [1] García-Marín, V., García-López, P. and Freire, M., Cajal’s contributions to glia research, *Trends in Neurosciences*, vol. 30:(9), 479–487 (2007)
- [2] Rouach, N., Astroglial metabolic networks sustain hippocampal synaptic transmission, *Science*, vol. 5, 1551–1555 (2008)
- [3] Vijayaraghavan, S., Glial–Neuronal Interactions – Implications for Plasticity and Drug Addiction, *The AAPS journal*, vol. 11:(1), 123–132 (2009)
- [4] Perea, G. and Araque, A., GLIA modulates synaptic transmission, *Brain Research Reviews*, vol. 63:(1), 93–102, (2010)
- [5] Dallérac, G., Chever, O. and Rouach, N., How do astrocytes shape synaptic transmission? Insights from electrophysiology, *Frontiers in Cellular Neuroscience*, vol. 7, 159, (2013)
- [6] Chever, O., Dossi, E., Pannasch, U., Derangeon, M. and Rouach, N., Astroglial networks promote neuronal coordination, *Science Signaling*, vol. 9:(410), ra6–ra6, (2016)
- [7] Bindocci, E., Savtchouk, I., Liaudet, N., Becker, D., Carriero, G. and Volterra, A., Three-dimensional  $\text{Ca}^{2+}$  imaging advances understanding of astrocyte biology, *Science*, vol. 356:(6339), (2017)

- [8] Pfrieger, F. W. and Barres, B. A., Synaptic Efficacy Enhanced by Glial Cells in Vitro, *Science*, vol. 277:(5332), 1684–1687 (1997)
- [9] Perea, G., Navarrete, M. and Araque, A., Tripartite synapses: astrocytes process and control synaptic information, *Trends in Neurosciences*, vol. 32:(8), 421–431, (2009)
- [10] Pérez-Alvarez, A. and Araque, A., Astrocyte-Neuron Interaction at Tripartite Synapses, *Current Drug Targets*, vol. 14:(11), 1220-1224, (2013)
- [11] Ben Achour, S. and Pascual, O., Glia: The many ways to modulate synaptic plasticity, *Neurochemistry International*, vol. 57:(4), 440–445 (2010)
- [12] Araque, A., Sanzgiri, R. P., Parpura, V. and Haydon, P. G., Calcium Elevation in Astrocytes Causes an NMDA Receptor-Dependent Increase in the Frequency of Miniature Synaptic Currents in Cultured Hippocampal Neurons, vol. 18:(17), 6822–6829, (1998)
- [13] Angulo, M. C., Kozlov, A. S., Charpak, S. and Audinat, E., Glutamate released from glial cells synchronizes neuronal activity in the hippocampus, *Journal of Neuroscience*, vol. 24:(31), 6920–6927 (2004)
- [14] Mansvelder, H. D. and McGehee, D. S., Cellular and synaptic mechanisms of nicotine addiction, *Journal of Neurobiology*, vol. 53:(4), 606–617 (2002)
- [15] Albuquerque, E. X., Pereira, Edna. F. R., Alkondon, M. and Rogers, S. W., Mammalian Nicotinic Acetylcholine Receptors: From Structure to Function, *Physiological Reviews*, vol. 89:(1), 73–120, (2009)
- [16] Stolerman, I. P., Mirza, N. R. and Shoaib, M., Nicotine psychopharmacology: Addiction, cognition and neuroadaptation, *Medicinal Research Reviews*, vol. 15, 47–72 (1995)
- [17] Levin, E. D. and Simon, B. B., Nicotinic acetylcholine involvement in cognitive function in animals, *Psychopharmacology*, vol. 138, 217–230 (1998)
- [18] Rezvani, A. H. and Levin, E. D., Cognitive effects of nicotine. *Biological Psychiatry*, vol. 49(3), 258–267 (2001)

- [19] Levin, E. D. and Rezvani, A. H., Nicotine treatment for cognitive dysfunction, *Curr Drug Targets CNS Neurol Disord*, vol. 1, 423–431 (2002)
- [20] Shepherd, G. M., *The synaptic organization of the brain*, Oxford University Press, Oxford (1990)
- [21] Carvalho, L. A. V., Modeling the thalamocortical loop, *International Journal of Bio-Medical Computing*, vol. 35, 267–296 (1994)
- [22] Madureira, D. Q. M., Carvalho, L. A. V. and Cheniaux, E., Attentional focus modulated by mesothalamic dopamine: consequences in parkinson’s disease and attention deficit hyperactivity disorder, *Cognitive Computation*, vol. 2, 31–49 (2010)
- [23] Mansvelder, H. D. and McGehee, D. S., Long-Term Potentiation of Excitatory Inputs to Brain Reward Areas by Nicotine, *Neuron*, vol. 27:(2), 349–357 (2000)
- [24] Dani, J. A. and Ji, D. and Zhou, F. M., Synaptic Plasticity and Nicotine Addiction, *Neuron*, vol. 31:(3), 349–352 (2001)
- [25] Placzek, A. N., Zhang, T. A. and Dani, J. A., Nicotinic mechanisms influencing synaptic plasticity in the hippocampus, *Acta Pharmacologica Sinica*, vol. 30:(6), 752–760, (2009)
- [26] Grundey, J., Thirugnanasambandam, N., Kaminsky, K., Drees, A., Skwirba, A. C., Lang, N., Paulus, W. and Nitsche, M. A., Rapid Effect of Nicotine Intake on Neuroplasticity in Non-Smoking Humans, *Frontiers in Pharmacology*, vol. 3, 186, (2012)
- [27] Morris, R. G. M., Toward a Representational Hypothesis of the Role of Hippocampal Synaptic Plasticity in Spatial and Other Forms of Learning, *Cold Spring Harbor Symposia on Quantitative Biology*, vol. 55, 161-173, (1990)
- [28] Malenka, R. C., Synaptic plasticity in the hippocampus: LTP and LTD, *Cell*, vol. 78:(4), 535–538, (1994)
- [29] Maren, S. and Baudry, M., Properties and Mechanisms of Long-Term Synaptic Plasticity in the Mammalian Brain: Relationships to Learning and Memory, *Neurobiology of Learning and Memory*, vol. 63:(1), 1–18, (1995)

- [30] Martin, S. J. and Morris, R. G. M., New life in an old idea: The synaptic plasticity and memory hypothesis revisited, *Hippocampus*, vol. 12:(5), 609–636, (2002)
- [31] Menachem-Zidon, O. B., Avital, A., Ben-Menahem, Y., Goshen, I., Kreisel, T., Shmueli, E. M., Segal M., Hur, T. B. and Yirmiya, R., Astrocytes support hippocampal-dependent memory and long-term potentiation via interleukin-1 signaling, *Brain, Behavior, and Immunity*, vol. 25:(5), 1008–1016, (2011)
- [32] Newman, L. A., Korol, D. L. and Gold, P. E., Lactate Produced by Glycogenolysis in Astrocytes Regulates Memory Processing, *PLoS ONE*, vol. 6:(12), e28427, (2011)
- [33] López-Hidalgo, M., Salgado-Puga, K., Alvarado-Martínez, R., Medina, A. C., Prado-Alcalá, R. A. and García-Colunga, J., Nicotine Uses Neuron-Glia Communication to Enhance Hippocampal Synaptic Transmission and Long-term Memory, *PLoS ONE*, vol. 7:(11), e49998, (2012)
- [34] McCall, M. A., Gregg, R. G., Behringer, R. R., Brenner, M., Delaney, C. L., Galbreath, E. J., Zhang, C. L., Pearce, R. A., Chiu, S. Y. and Messing, A., Targeted deletion in astrocyte intermediate filament (*Gfap*) alters neuronal physiology, *Proceedings of the National Academy of Sciences of the United States of America*, vol. 93:(13), 6361–6366, (1996)
- [35] Shibuki, K., Gomi, H., Chen, L., Bao, S., Kim, J. J., Wakatsuki, H., Fujisaki, T., Fujimoto, K., Katoh, A., Ikeda, T., Chen, C., Thompson, R. F. and Itohara, S., Deficient Cerebellar Long-Term Depression, Impaired Eyeblink Conditioning, and Normal Motor Coordination in GFAP Mutant Mice, *Neuron*, vol. 16:(3), 587–599, (1996)
- [36] Fellin, T., Pascual, O., Gobbo, S., Pozzan, T., Haydon, P. G. and Carmignoto, G., Neuronal Synchrony Mediated by Astrocytic Glutamate through Activation of Extrasynaptic NMDA Receptors, *Neuron*, vol. 43:(5), 729–743, (2004)
- [37] Guimarães, K., Madureira, D.Q.M., Madureira, A.L., The Reward-Attention Circuit Model: Nicotine’s Influence on Attentional Focus and Consequences on ADHD, *Neurocomputing*, vol. 242, 140–149, (2017)

- [38] Wise, R. A., Brain Reward Circuitry: Insights from Unsesed Incentives, *Neuron*, vol. 36, 229–240, (2002)
- [39] Nadkarni, S. and Jung, P., Dressed neurons: modeling neural–glial interactions, *Physical Biology*, vol. 1:(1), 35–41, (2004)
- [40] Volman, V., Ben-Jacob, E. and Levine, H., The Astrocyte as a Gatekeeper of Synaptic Information Transfer, *Neural Computation*, vol. 19:(2), 303–326, (2007)
- [41] De Pittà, M., Goldberg, M., Volman, V., Berry, H. and Ben-Jacob, E., Glutamate regulation of calcium and IP3 oscillating and pulsating dynamics in astrocytes, *Journal of Biological Physics*, vol. 35:(4), 383–411, (2009)
- [42] Li, YX. and Rinzel, J., Equations for InsP3 Receptor-mediated  $[Ca^{2+}]_i$  Oscillations Derived from a Detailed Kinetic Model: A Hodgkin-Huxley Like Formalism, *Journal of Theoretical Biology*, vol. 166:(4), 461–473, (1994)
- [43] Porter, J. T. and McCarthy, K. D., Hippocampal Astrocytes In Situ Respond to Glutamate Released from Synaptic Terminals, *The Journal of Neuroscience*, vol. 16:(16), 5073–5081, (1996)
- [44] Gerstner W. and Kistler W. M., Spiking neuron models: single neurons, populations, plasticity, Cambridge UK: Cambridge University Press, 94–105, (2002)
- [45] Ermentrout, G. B. and Terman, David H., Mathematical foundations of neuroscience, *Interdisciplinary Applied Mathematics*, Springer, New York, vol. 35, (2010)
- [46] MacGregor, R. J., Neural and brain modeling, San Diego: Academic Press Incorporation, (1987)
- [47] MacGregor, R. J. and Oliver, R. M., A model for repetitive firing in neurons, *Biol Cybern*, vol. 16, 53–64, (1974)
- [48] Carvalho, L. A. V. and Roitman, V. L., A computational model for the neurobiological substrates of visual attention, *International Journal of Bio-Medical Computing*, vol. 38, 33–45, (1995)

- [49] Parri, H. R. and Gould, T. M. and Crunelli, V., Spontaneous astrocytic  $\text{Ca}^{2+}$  oscillations in situ drive NMDAR-mediated neuronal excitation, *Nature Neuroscience*, vol. 4:(8), 803–812, (2001)
- [50] Haydon, P. G. and Carmignoto, G., Astrocyte Control of Synaptic Transmission and Neurovascular Coupling, *Physiological Reviews*, vol. 86:(3), 1009–1031, (2006)
- [51] Papouin, T. and Oliet, S. H. R., Organization, control and function of extrasynaptic NMDA receptors, *Philosophical Transactions of the Royal Society of London B: Biological Sciences*, vol. 369:(1654), (2014)
- [52] Araque, G. Carmignoto and P. G. Haydon, Dynamic signaling between astrocytes and neurons, *Annual Review of Physiology*, vol. 63:(1), 795–813, (2001)
- [53] B. W. Connors and M. J. Gutnick and D. A. Prince, Electrophysiological properties of neocortical neurons in vitro, *Journal of Neurophysiology*, vol. 48:(6), 1302–1320, (1982)
- [54] D. A. McCormick and B. W. Connors and J. W. Lighthall and D. A. Prince, Comparative electrophysiology of pyramidal and sparsely spiny stellate neurons of the neocortex, *Journal of Neurophysiology*, vol. 54:(4), 782–806, (1985)